Hubble Space Telescope Advanced Camera for Surveys Imaging of ω Centauri: Optical Counterpart for the Quiescent Low#Mass X#Ray Binary

The Astrophysical Journal, 613:512–516, 2004 September 20

HUBBLE SPACE TELESCOPE ADVANCED CAMERA FOR SURVEYS IMAGING OF ω CENTAURI: OPTICAL COUNTERPART FOR THE QUIESCENT LOW-MASS X-RAY BINARY[1]

Daryl Haggard,[2,3] Adrienne M. Cool,[2] Jay Anderson,[4] Peter D. Edmonds,[5] Paul J. Callanan,[6]
Craig O. Heinke,[5] Jonathan E. Grindlay,[5] and Charles D. Bailyn[7]
Received 2003 December 22; accepted 2004 April 2

ABSTRACT

We report the discovery of an optical counterpart to a quiescent neutron star in the globular cluster ω Centauri (NGC 5139). The star was found as part of our wide-field imaging study of ω Cen using the Advanced Camera for Surveys (ACS) on the *Hubble Space Telescope*. Its magnitude and color ($R_{625} = 25.2$, $B_{435} - R_{625} = 1.5$) place it more than 1.5 mag to the blue side of the main sequence. Through an Hα filter it is ~1.3 mag brighter than cluster stars of comparable R_{625} magnitude. The blue color and Hα excess suggest the presence of an accretion disk, implying that the neutron star is accreting from a binary companion and is thus a quiescent low-mass X-ray binary. If the companion is a main-sequence star, then the faint absolute magnitude ($M_{625} \simeq 11.6$) constrains it to be of very low mass ($M \lesssim 0.14\ M_{\odot}$). The faintness of the disk ($M_{435} \sim 13$) suggests a very low rate of accretion onto the neutron star. We also detect 13 probable white dwarfs and three possible BY Draconis stars in the $20'' \times 20''$ region analyzed here, suggesting that a large number of white dwarfs and active binaries will be observable in the full ACS study.

Subject headings: globular clusters: individual (NGC 5139) — stars: neutron — techniques: photometric — white dwarfs — X-rays: binaries

1. INTRODUCTION

ω Centauri is a prime target for studies of stellar collisions. It is nearby ($D \simeq 5$ kpc), massive, and despite a relatively moderate central density has one of the highest predicted rates of stellar interactions among globular clusters, owing to its very large core. Channels for compact binary production include exchange encounters, binary-binary collisions, and possibly tidal capture (Hut et al. 1992; Fregeau et al. 2003, and references therein). Di Stefano & Rappaport (1994) predicted that ~100 cataclysmic variables (CVs) formed by tidal capture should be in ω Cen at present. Some compact binaries may also evolve directly from primordial binaries in this cluster (Davies 1997).

We are using the *Chandra X-Ray Observatory* and the Advanced Camera for Surveys (ACS) on the *Hubble Space Telescope* (*HST*) to search for compact binary stars in ω Cen. The nine fields observed with ACS form a mosaic that encompasses more than 100 of the *Chandra* sources identified with ACIS-I in the direction of ω Cen (Cool et al. 2002). The ACS mosaic contains over a million stars and represents the most complete census of stars in ω Cen yet obtained.

Here we report the first detection of an optical counterpart for a *Chandra* source using the ACS data. The source in question was identified as a possible transient neutron star in quiescence by Rutledge et al. (2002) in a spectral analysis of 32 of the brightest sources in the *Chandra* data. Its X-ray spectrum was found to be consistent with thermal emission from a neutron star with a hydrogen atmosphere and inconsistent with several other possible explanations. The characteristics of the optical counterpart that we have identified suggest the presence of a disk and binary companion, as in a quiescent low-mass X-ray binary (qLMXB). While more than two dozen qLMXBs have been identified in 10 different globular clusters from their X-ray spectra (Heinke et al. 2003b), this is only the second optical counterpart found for one of these objects during quiescence (the other being X5 in 47 Tuc; Edmonds et al. 2002). qLMXBs are believed to play an important role in the production of millisecond pulsars; studying them in globular clusters also holds the promise of new constraints on neutron star equations of state (Brown et al. 1998; Heinke et al. 2003a).

We describe the ACS observations and our astrometric and photometric analyses in § 2. In § 3 we present the proposed optical counterpart and discuss it in § 4. Results of our search for additional optical counterparts to *Chandra* sources, as well as our study of stellar populations in ω Cen using the ACS data, will appear in subsequent papers.

2. OBSERVATIONS AND ANALYSIS

The ACS observations were made on 2002 June 27–29. They consist of a 3×3 mosaic of nine pointings with the Wide Field Camera (WFC) covering about $10' \times 10'$, out to beyond ω Cen's half-light radius ($r_h = 288''$; Harris 1996). The X-ray source of interest here lies ~4.′5 west of the cluster center. At each of the pointings we obtained three 340 s exposures with the F625W (R_{625}) and F435W (B_{435}) filters and four 440 s exposures with the F658N (Hα) filter, shifting the camera between exposures to fill the chip gap. Having three to four exposures per filter

[1] Based on observations with the NASA/ESA *Hubble Space Telescope* obtained at the Space Telescope Science Institute, which is operated by the Association of Universities for Research in Astronomy, Incorporated, under NASA contract NAS5-26555.

[2] Department of Physics and Astronomy, San Francisco State University, 1600 Holloway Avenue, San Francisco, CA 94618; cool@sfsu.edu.

[3] Department of Astronomy, University of Washington, Box 351580, Seattle, WA 98195; dhaggard@astro.washington.edu.

[4] Department of Physics and Astronomy, Rice University, 6100 Main Street, Houston, TX 77005; jay@eeyore.rice.edu.

[5] Harvard-Smithsonian Center for Astrophysics, 60 Garden Street, Cambridge, MA 02138; pedmonds@cfa.harvard.edu, cheinke@cfa.harvard.edu, josh@ cfa.harvard.edu.

[6] Department of Physics, University College Cork, Ireland; paulc@ucc.ie.

[7] Department of Astronomy, Yale University, New Haven, CT 06520; bailyn@astro.yale.edu.

TABLE 1
ASTROMETRY

Source (1)	*Chandra* R.A. (J2000.0) (2)	*Chandra* Decl. (J2000.0) (3)	Optical−X-Ray, Raw $\Delta\alpha$, $\Delta\delta$ (arcsec, arcsec) (4)	Optical−X-Ray, Corrected $\Delta\alpha'$, $\Delta\delta'$ (arcsec, arcsec) (5)	*HST* Archival Image, Chip (6)	Pixel Coordinates (x, y) (7)
XA	13 26 52.141	−47 29 35.63	−0.08, 0.31	−0.03, 0.02	j6lp05vsq, 1	323, 864
XB	13 26 53.513	−47 29 00.37	−0.02, 0.28	0.03, −0.02	j6lp05vsq, 1	1005, 1194
XC	13 26 48.656	−47 27 44.88	0.00, 0.33	0.05, 0.04	j6lp05vsq, 1	2682, 280
qLMXB	13 26 19.795	−47 29 10.64	0.19, 0.35	0.24, −0.05	j6lp02ffq, 2	1828, 325

NOTE.—Units of right ascension are hours, minutes, and seconds, and units of declination are degrees, arcminutes, and arcseconds.

enables us to recognize and eliminate false detections and poor measurements caused by cosmic rays. One short exposure in each of R_{625} and B_{435} was also taken to fill out the cluster's horizontal and giant branches. We use these filters to look in the X-ray error circle for stars that are blue and/or Hα-bright as potential signatures of accretion.

2.1. *Astrometry*

Chandra coordinates determined using *wavdetect*[8] for the quiescent neutron star identified by Rutledge et al. (2002) and for three previously known X-ray sources in the core, are given in Table 1, columns (2) and (3). To map these positions onto the ACS/WFC images, we first applied a distortion correction to the individual WFC images using the solution obtained for the B_{475} filter from a study of 47 Tuc (Anderson 2002). This solution should be accurate to ~0.15 WFC pixel (1 WFC pixel = 0\".05). We then stitched together all the individual B_{435} frames to make a mosaic of the entire field. The images fit together well, with no sign of misaligned star images where chips overlap, indicating that the distortion correction is working well.

To determine the right ascension and declination associated with stars on the mosaic, we used the star lists of Kaluzny et al. (1996) and van Leeuwen et al. (2000). More than 15,000 of the former and 4000 of the latter fall within the field of view of our mosaic. There is a small zero-point offset of 0\".5 between the two systems, which we take to be indicative of the uncertainty in the absolute frame; we used the Kaluzny system to define the transformation between our mosaic system and right ascension and declination. We estimate that the transformation is accurate to ≲0\".4 over the entire mosaic.

We cross-checked the optical coordinates using counterparts previously identified in *HST* WFPC2 images for two *ROSAT* sources in the cluster core, XA and XB. We recovered stars A and B that Carson et al. (2000) identified as CVs, and confirmed that both are Hα-bright and blue in the ACS/WFC images (Haggard et al. 2002). The differences between our optical positions for these two stars and the *Chandra* positions (Table 1, col. [4]) are well within the 0\".6 uncertainty (90% confidence) in *Chandra*'s absolute coordinate system.

Noting that the X-ray positions for stars A and B are offset from their optical positions in nearly the same direction, we used them to improve the placement of the other X-ray sources on the ACS mosaic. We shifted the X-ray positions northwest by $(\Delta\alpha, \Delta\delta) = (-0\rlap{.}''05, 0\rlap{.}''30)$. This shift places star C, identified by Carson et al. (2000) as a tentative counterpart of the third *ROSAT* core source, XC, just $\Delta r' = 0\rlap{.}''06$ from the corresponding *Chandra* source position (Table 1, col. [5]), confirming that it is the likely source of the X-rays. Star C is Hα-bright but not blue; it may be either a BY Dra–type active binary or a cataclysmic variable.

The effect of this boresight correction on the position of the X-ray error circle for the qLMXB is shown in Figure 1. The remaining uncertainty in the position of the qLMXB is likely to be dominated by the uncertainty in off-axis *wavdetect* positions, ~0\".5 at the 4'.5 off-axis angle of the object in the *Chandra* ACIS-I observation (Feigelson et al. 2002). An additional uncertainty of up to ~0\".4 associated with the construction of the ACS mosaic and the large separation between the qLMXB and stars A and B may also be present. We therefore adopted a 1\" error circle in the search for its optical counterpart.

2.2. *Photometry*

In view of the variability of the point spread function (PSF) in the ACS/WFC (Krist 2003), we extracted a 400 × 400 pixel

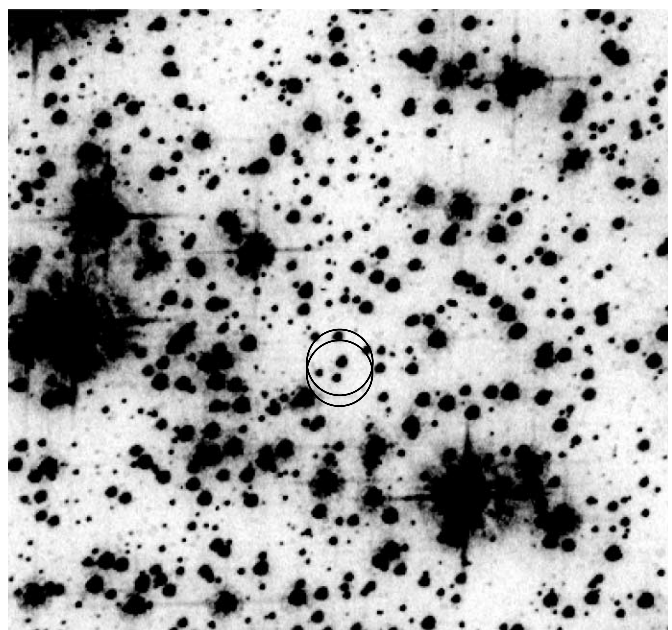

FIG. 1.—The 20\" × 20\" region used in the search for the optical counterpart to the qLMXB in the B_{435} filter. North is up and east is to the left, approximately. This field is roughly 4'.5 west of the cluster center. Pre- and post-boresight correction 1\" radius X-ray error circles are shown (*bottom and top circles, respectively*).

[8] See http://asc.harvard.edu/ciao.

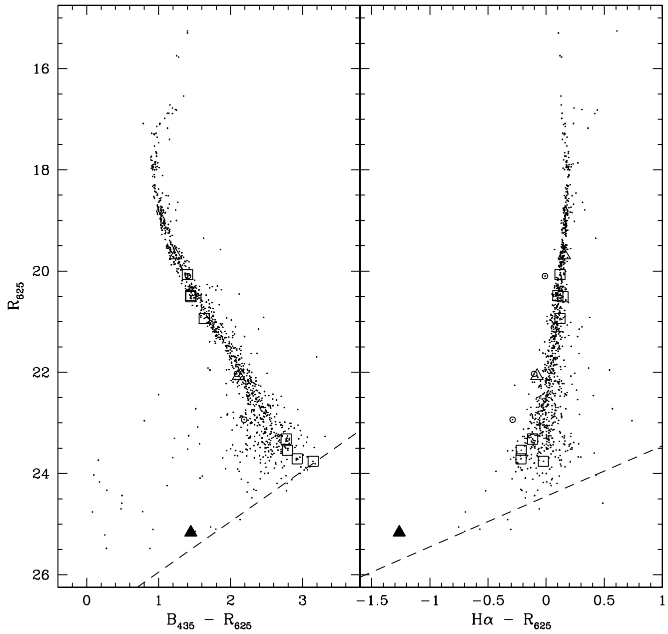

FIG. 2.—CMDs for stars in the region shown in Fig. 1. Median magnitudes are plotted for stars detected in all three R_{625} and all three B_{435} images. Sources within 0″.5 and 1″.0 of the boresight-corrected X-ray source position are indicated as triangles and squares, respectively. The proposed optical counterpart to the qLMXB is distinctly blue and Hα-bright (*filled triangle*). Three BY Dra candidates are also detected (*small circles*). Approximate magnitude limits are indicated with dashed lines. Several probable white dwarfs are visible in the lower left of the left-hand panel.

area ($\sim 20'' \times 20''$) approximately centered on the *Chandra* source position from each of the 12 images (Fig. 1). We used DAOPHOT (Stetson 1987) for the analysis, as the crowding is significant even outside the cluster core. We selected $\sim$10 bright, isolated, unsaturated stars to characterize the PSF. As it demonstrated little or no variability across this small region, we adopted a constant model. The best results were obtained by making a separate PSF for each image.

We obtained a preliminary star list using DAOPHOT/FIND and then examined and compared the images by eye in order to remove cosmic rays and other spurious detections. We also manually added to the star list near neighbors revealed in the course of PSF fitting. Magnitudes and positions for the 1454 stars identified in this way were then obtained using DAOPHOT/ALLSTAR for each image independently. Finally, we matched up stars measured in each of the 10 long exposures, requiring that the positions match to within 1 pixel. We also analyzed the images using ALLFRAME (Stetson 1994), which is designed to use consistent positions for stars in all images. ALLSTAR gave better results, apparently because of the difficulty in transforming star positions between non-aligned exposures with sufficient accuracy, due to the large distortion in the WFC. Here we report results obtained using ALLSTAR, which we have calibrated using "vegamag" zero points kindly provided by Sirianni et al. (2003).

3. RESULTS

Color-magnitude diagrams (CMDs) for the 1454 stars in the $20'' \times 20''$ field are shown in Figure 2. To reduce the effects of any remaining cosmic rays, we have plotted median magnitudes. Stars are shown if they appear in all three R_{625} and all three B_{435} images and any number of Hα images. This ensures that blue stars (e.g., white dwarfs) are not overlooked, even if they are too faint to be detected in Hα.

In the $B_{435} - R_{625}$ versus R_{625} diagram (Fig. 2, *left panel*), the main sequence can be seen extending $\gtrsim$6 mag below the turnoff and about a dozen white dwarfs are visible at the lower left from $R_{625} \simeq 23.5$–25.5 and $B_{435} - R_{625} \simeq 0$–$1$. In the right panel we plot $H\alpha - R_{625}$ versus R_{625}. Here the main sequence appears nearly vertical and has been shifted so that it is approximately centered on $H\alpha - R_{625} = 0$. In both diagrams, stars within 0″.5 and 1″.0 of the boresight-corrected *Chandra* position are indicated with triangles and squares, respectively.

The most interesting star in the X-ray error circle is shown as a filled triangle in Figure 2. The star is very faint, at $R_{625} = 25.2$ and $B_{435} - R_{625} = 1.5$, and would not have been detected in B_{435} or Hα were it not considerably blue and Hα-bright. It is $\gtrsim$1.5 mag bluer than the main sequence and noticeably redder than white dwarfs of comparable brightness. In the $H\alpha - R_{625}$ diagram, the star lies $\sim$1.3 mag to the left of the main sequence, suggesting the presence of a strong emission line. Despite being so faint, the star was found in all 10 images by the automated DAOPHOT/FIND routine, making it one of the most reliable detections with $R_{625} > 25$. No other star in the 1″ error circle is significantly blue or Hα bright. We identify this star as the probable optical counterpart of the X-ray source.

A finding chart for the proposed optical counterpart is shown in Figure 3. It lies just $\Delta r' = 0''.25$ from the boresight-corrected X-ray position (Table 1, col. [5]). Even without any

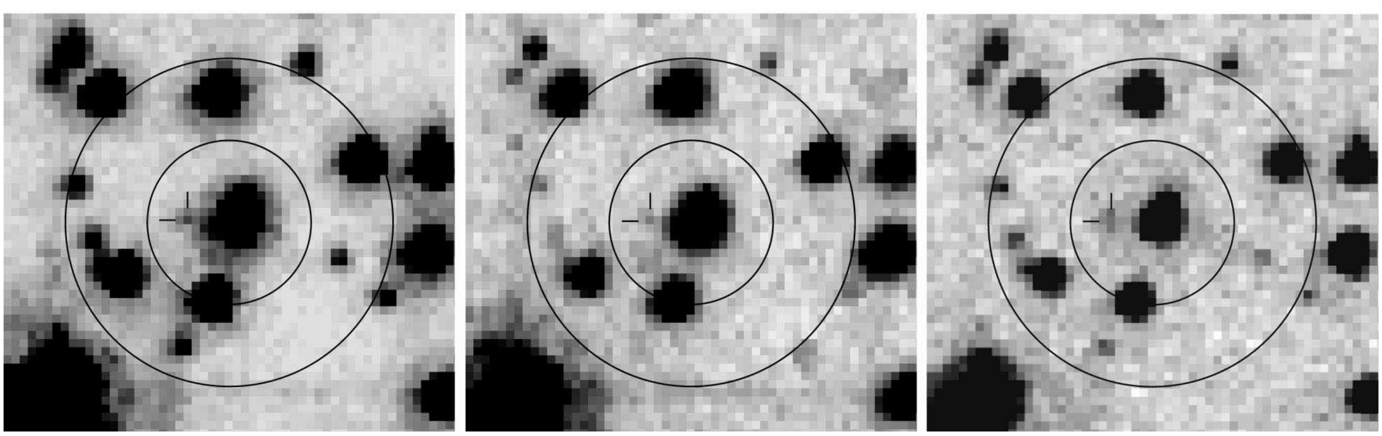

FIG. 3.—Finding chart for the proposed optical counterpart to the qLMXB (see crosshairs) in R_{625} (*left*), B_{435} (*middle*), and Hα (*right*) filters. These images are averages of the three or four available exposures in each filter. Error circles of radius 0″.5 and 1″.0 centered on the boresight-corrected position are shown.

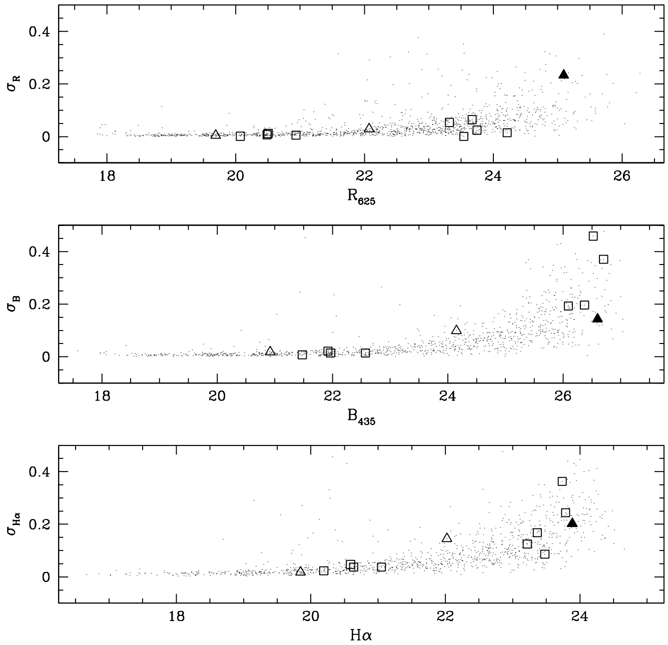

FIG. 4.—Plot of σ vs. median magnitude for the R_{625}, B_{435} and Hα filters. Detection in all of the "long" exposures in a given filter was required for inclusion in the corresponding plot. Symbols are as in Fig. 2. Values of σ measured for the proposed optical counterpart are consistent with being due to measurement uncertainties alone.

boresight correction, the X-ray and optical positions are offset by 0''.40 (Table 1, col. [4])—well within the $\sim$1'' uncertainty of *HST* and *Chandra* absolute positions. That the agreement between the optical and X-ray positions improves after the boresight correction further supports the identification of this star as the optical counterpart.

We performed several further tests to check the reality of this faint object and the reliability of the measured magnitudes. First, we examined the star visually in each of the 10 long-exposure images, and verified that no cosmic rays had affected the photometry. In CMDs made from averaged instead of medianed magnitudes, the star appears in similar locations. Comparable results were also obtained using ALLFRAME, which is somewhat less susceptible to contamination of faint star magnitudes by bright neighbors. This is reassuring, since the candidate has a neighbor just 0''.3 (6 pixels) away that is $\sim$5.5 mag brighter in R_{625} (Fig. 3). We also examined the residuals in the vicinity of the star after subtracting it out of each of the images and found that the subtractions were clean, with no sign of any flux being left behind. Thus the object appears to be stellar.

As a final test, we computed standard deviations for magnitudes measured in each filter (Fig. 4). These plots give an indication of the accuracy of the photometry as a function of magnitude and also show that, in all filters, the star is $\gtrsim$0.5 mag brighter than the faintest stars detected. The accuracy with which it is measured ($\sigma \lesssim 0.2$ mag in all filters) implies that unusual $B_{435} - R_{625}$ and H$\alpha - R_{625}$ colors are clearly significant. That the star is blue and Hα-bright relative to other stars of comparable R_{625} magnitude can also be verified visually (Fig. 3).

4. DISCUSSION

The star we have identified as the optical counterpart of the qLMXB is faint, blue, and Hα-bright. These characteristics are typical of semidetached binaries in which a compact object is accreting from a low-mass companion (e.g., Cool et al. 1998). From the observed 1.3 mag Hα excess and the widths of the F658N and F675W filters, we infer the presence of an emission line with an equivalent width of EW(Hα) $\simeq$ 220 Å, after correcting for the contribution of the line to the flux through the R_{625} filter. Such a strong line is reminiscent of lines seen in short-orbital-period cataclysmic variables with low accretion rates (Patterson 1984; Tylenda 1981). Comparably strong Hα emission is also seen in the soft X-ray transient GRO J0422+32, a black hole candidate with $P_{\rm orb} \sim 5$ hr (Harlaftis et al. 1999). Whereas in principle the neutron star might have been accreting from the cluster interstellar medium (Rutledge et al. 2002), the characteristics of the optical counterpart strongly suggest the presence of an accretion disk and a low-mass binary companion.

The object's X-ray to optical flux ratio is high compared to qLMXBs in the field but is on the order of those detected or constrained optically in globular clusters. Assuming a $V - R$ color of $\sim$0.5, we estimate $f_X/f_V \sim 240$ for this object. Similar estimates for the two qLMXBs in 47 Tuc yield $f_X/f_V \sim 50$ for X5 and a lower limit of $f_X/f_V \gtrsim 180$ for X7 (the latter based on a limit on the brightness of the optical counterpart; Heinke et al. 2003; Edmonds et al. 2002). Our limit on the magnitude of the optical counterpart of the qLMXB in NGC 6397 implies $f_X/f_V \gtrsim 50$ (Grindlay et al. 2001). Field qLMXBs Aql X-1, Cen X-4 and SAX J1808 have $f_X/f_V \sim 10$–20 judging from information given by Campana et al. (1998), Chevalier et al. (1989, 1999), and Homer et al. (2001).

Further insight can be gained from the intrinsic color and absolute magnitude of the optical counterpart. Adopting a reddening of $E(B - V) = 0.11$ (Lub 2002), we derive extinction values of $A_{435} = 0.45$ and $A_{625} = 0.29$ and thus an intrinsic color of $(B_{435} - R_{625})_0 = 1.3$. This color helps to rule out the possibility raised by Rutledge et al. (2002) that the source could be a narrow-line Seyfert I galaxy. For a plausible spectrum, it corresponds to a Sloan $g' - r'$ color of $\sim$1.0, which is redder than 150 such galaxies studied by Williams et al. (2002). The high f_X/f_V ratio further argues against it being an active galaxy, as active galactic nuclei typically have f_X/f_V values 1–2 orders of magnitude lower (e.g., Koekemoer et al. 2004), as does the excess Hα emission, since a strong line would have to be redshifted into the F658N bandpass by chance. A measurement of the object's proper motion would help confirm its cluster membership, which would also rule out the possibility that it is a field qLMXB along the line of sight to ω Cen. We estimate that a baseline of $\gtrsim$5 yr would be required to make such a measurement given the faintness of this object and the $\sim$6 mas yr^{-1} ($\sim$0.1 WFC pixels yr^{-1}) proper motion of ω Cen.

As a cluster member, the star is at $\sim$5.0 kpc. Using the extinction above, the distance modulus is then $(m - M)_{625} = 13.8$, yielding an absolute magnitude of $M_{625} = 11.4$. Adjusting for the Hα emission line within the F625W bandpass gives $M_{625} \simeq 11.6$ for the continuum alone. A $\pm$0.5 kpc uncertainty in the distance (cf. van Leeuwen et al. 2000 vs. Thompson et al. 2001) introduces an uncertainty of about $\pm$0.2 mag in these values.

This is the faintest optical counterpart detected for a qLMXB. The only known system that may be fainter is the one in NGC 6397, for which a limit of $M_V > 11$ has been derived from its nondetection in *HST* WFPC2 images (Grindlay et al. 2001). The optical counterpart to X5 in 47 Tuc and to the field qLMXBs Aql X-1 and Cen X-4 (M_V = 8.2, 8.1, and 7.5–8.5, respectively; Edmonds et al. 2002 and references therein) are all considerably brighter. Such a faint absolute magnitude implies either that the secondary star is of very low mass or that it is a compact star. In the case of a main-sequence secondary, we can obtain an upper limit to the mass by assuming that it provides all the light in the R_{625} band. For the metallicity of ω Cen, an absolute magnitude of $M_{625} = 11.6$ corresponds to a zero-age main sequence (ZAMS) star with a mass of $\sim 0.14\ M_{\odot}$ (Baraffe et al. 1997). Such a star would contribute about 20% of the light in the B_{435} band, leaving a disk with $M_{435} \simeq 13.1$.

We cannot place a lower limit on the mass of the secondary star. However, the intrinsic color of the system is sufficiently red, despite its location blueward of the main sequence, that it appears likely that at least some, if not all, of the light in the R_{625} band comes from the secondary. To account for its color with a power-law spectrum from a disk alone would require a positive exponent: $f_{\lambda} \sim \lambda^{0.15}$. A more typical disk spectrum scaling as λ^{-2} would have an intrinsic color of $(B_{435} - R_{625})_0 \sim 0.2$ and account for only $\sim$40% of the light in the R_{625} band, even if all the B_{435} flux were from the disk. The remaining R_{625}-band light could be accounted for by a main-sequence star of mass $\sim 0.12\ M_{\odot}$. The difficulty of accounting for the object's color without a significant contribution from the secondary star argues against the possibility that the secondary is compact.

A main-sequence secondary star mass of $\lesssim 0.12$–$0.14\ M_{\odot}$ implies a short orbital period for the system. In particular, for a ZAMS star in this mass range to fill its Roche lobe would require an orbital period of $\lesssim$1.2–1.5 hr (Warner 1995); longer periods are possible if the star is underdense (e.g., Edmonds et al. 2002; Kaluzny & Thompson 2003).

The disk in the system must also be intrinsically very faint, with $M_{435} \sim 13$. This is considerably fainter than even the disk in SAX J1808.4$-$3658, a transient with a 2 hr period, whose disk is estimated at $M_B = 5.7$–9.0 (Homer et al. 2001). Disks this faint are seen in CVs with periods below the period gap, i.e., $\lesssim$2 hr (e.g., Sproats et al. 1996), with mass transfer rates of order of $10^{-11}\ M_{\odot}\ \mathrm{yr}^{-1}$ driven by gravitational radiation (Warner 1995). That an accreting neutron star with a potential well a factor of $\sim$1000 larger would have such a faint disk suggests an extremely low rate of accretion onto the neutron star at present, on the order of $10^{-14}\ M_{\odot}\ \mathrm{yr}^{-1}$. This is significantly lower than the rate driven by gravitational radiation, if indeed the system has a short orbital period. A possible explanation for this apparent discrepancy could be that material is being transferred to the disk from the secondary, but that little, if any, is accreting onto the neutron star from the disk at the present time. Such a picture would fit with the scenario proposed by Rutledge et al. (2002), in which the observed X-ray emission arises from the neutron star itself, and not from present-day accretion. In the Brown et al. (1998) model, deep crustal heating of the neutron star's core occurs during transient accretion events; a time-averaged mass transfer rate of $\sim 8 \times 10^{-12}\ M_{\odot}\ \mathrm{yr}^{-1}$ is required to explain the current X-ray luminosity of the neutron star in this system. We observe no variability in the optical flux ($\lesssim$0.2 mag, 1 σ; Fig. 4), which is also consistent with little or no current accretion onto the neutron star. However, the constraints we place are limited by the faintness of the star, the small number of exposures in each filter and the short ($\sim$1.5 hr) time span of the observations.

Finally, we note that several other stars of interest appear in the CMD in Figure 2. Three stars appear mildly Hα-bright in the right panel but are on or near the main sequence in the left panel (*small circles*). Visual inspections suggest the stars are well measured. These may be BY Dra–type active stars as have been seen, e.g., in NGC 6397 (Taylor et al. 2001). About a dozen faint blue stars with $B_{435} - R_{625} \lesssim 1$ and $R_{625} \gtrsim 23.5$ are probable white dwarfs. Finding such a large number in this small region suggests that several thousand white dwarfs should be detected in the full ACS mosaic.

We gratefully acknowledge discussions with Scott Anderson and thank Marco Sirianni for providing ACS/WFC calibration information in advance of publication. This work was supported by NASA grant HST-GO-9442.

REFERENCES

Anderson, J. 2002, in The 2002 *HST* Calibration Workshop, ed. S. Arribas, A. Koekemoer, & B. Whitmore (Baltimore: STScI), 13
Baraffe, I., Chabrier, G., Allard, F., & Hauschildt, P. H. 1997, A&A, 327, 1054
Brown, E. F., Bildsten, L., & Rutledge, R. E. 1998, ApJ, 504, L95
Campana S., Colpi, M., Mereghetti, S., Stella, L., & Tavani, M. 1998, A&A Rev., 8, 279
Carson, J. E., Cool, A. M., & Grindlay, J. E. 2000, ApJ, 532, 461
Chevalier, C., Ilovaisky, S. A., Leisy, P., & Patat, F. 1999, A&A, 347, L51
Chevalier, C., Ilovaisky, S. A., van Paradijs, J., Pedersen, H., & van der Klis, M. 1989, A&A, 210, 114
Cool, A. M., Grindlay, J. E., Cohn, H. N., Lugger, P. M., & Bailyn, C. D. 1998, ApJ, 508, L75
Cool, A. M., Haggard, D., & Carlin, J. L. 2002, in ASP Conf. Ser. 265, Omega Centauri, A Unique Window into Astrophysics, ed. F. van Leeuwen, J. D. Hughes, & G. Piotto (San Francisco: ASP), 277
Davies, M. B. 1997, MNRAS, 288, 117
Di Stefano, R., & Rappaport, S. 1994, ApJ, 423, 274
Edmonds, P. D., Heinke, C. O., Grindlay, J. E., & Gilliland, R. L. 2002, ApJ, 564, L17
Feigelson, E. D., Broos, P., Gaffney, J. A., Garmire, G., Hillenbrand, L. A., Pravdo, S. H., Townsley, L., & Tsuboi, Y. 2002, ApJ, 574, 258
Fregeau, J. M., Gurkan, M. A., Joshi, K. J., & Rasio, F. A. 2003, ApJ, 593, 772
Grindlay, J. E., Heinke, C. O., Edmonds, P. D., Murray, S. S., & Cool, A. M. 2001, ApJ, 563, L53
Haggard, D., Fuller, A. D., Dorfman, J. L., Cool, A. M., Anderson, J., Edmonds, P. E., & Davies, M. B. 2002, BAAS, 34, 1104
Harlaftis, E., Collier, S., Horne, K., & Filippenko, A. V. 1999, A&A, 341, 491
Harris, W. E. 1996, AJ, 112, 1487
Heinke, C. O., Grindlay, J. E., Lloyd, D. A., & Edmonds, P. D. 2003a, ApJ, 588, 452
Heinke, C. O., Grindlay, J. E., Lugger, P. M., Cohn, H. N., Edmonds, P. D., Lloyd, D. A., & Cool, A. M. 2003b, ApJ, 598, 501
Homer, L., Charles, P. A., Chakrabarty, D., & van Zyl 2001, MNRAS, 325, 1471
Hut, P., et al. 1992, PASP, 104, 981
Kaluzny, J., Kubiak, M., Szymanski, M., Udalski, A., Krzeminski W., & Mateo, M. 1996, A&AS, 120, 139
Kaluzny, J., & Thompson, I. B. 2003, AJ, 125, 2534
Koekemoer, A. M., et al. 2004, ApJ, 600, L123
Krist, J. 2003, ACS WFC and HRC Field-Dependent PSF Variations Due To Optical and Charge Diffusion Effects (ACS ISR 03-06; Baltimore: STScI), http://www.stsci.edu/hst/acs/documents/isrs/isr0306.pdf
Lub, J. 2002, in ASP Conf. Ser. 265, Omega Centauri, A Unique Window into Astrophysics, ed. F. van Leeuwen, J. D. Hughes, & G. Piotto (San Francisco: ASP), 95
Patterson, J. 1984, ApJS, 54, 443
Rutledge, R. E., Bildsten, L., Brown, E. F., Pavlov, G. G., & Zavlin, V. E. 2002, ApJ, 578, 405
Sirianni, M., et al. 2003, BAAS, 35, 722
Sproats, L. N., Howell, S. B., & Mason, K. O. 1996, MNRAS, 282, 1211
Stetson, P. B. 1987, PASP, 99, 191
———. 1994, PASP, 106, 250
Taylor, J. M., Grindlay, J. E., Edmonds, P. D., & Cool, A. M. 2001, ApJ, 553, L169
Thompson, I. B., Kaluzny, J., Pych, W., Burley, G., Krzeminski, W., Paczynski, B., Persson, S. E., & Preston, G. W. 2001, AJ, 121, 3089
Tylenda, R. 1981, Acta Astron., 31, 127
van Leeuwen, F., Le Poole, R. S., Reijns, R. A., Freeman, K. C., & de Zeeuw, P. T. 2000, A&A, 360, 472
Warner, B. 1995, Cataclysmic Variable Stars (Cambridge: Cambridge Univ. Press)
Williams, R. J., Pogge, R. W., & Mathur, S. 2002, AJ, 124, 3042